Biochemical and Biophysical Research Communications 377 (2008) 23–28

Contents lists available at ScienceDirect

Biochemical and Biophysical Research Communications

journal homepage: www.elsevier.com/locate/ybbrc

Crystal structure of the Bruton's tyrosine kinase PH domain with phosphatidylinositol

Kazutaka Murayama [a,b], Miyuki Kato-Murayama [b], Chiemi Mishima [b], Ryogo Akasaka [b], Mikako Shirouzu [b], Yasuhisa Fukui [c,1], Shigeyuki Yokoyama [b,d,*]

[a] Graduate School of Biomedical Engineering, Tohoku University, 2-1 Seiryo-machi, Aoba-ku, Sendai 980-8575, Japan
[b] Systems and Structural Biology Center, Yokohama Institute, RIKEN, 1-7-22 Suehiro-cho, Tsurumi, Yokohama 230-0045, Japan
[c] Department of Applied Biological Chemistry, Graduate School of Agricultural and Life Sciences, The University of Tokyo, 1-1-1 Yayoi, Bunkyo-ku, Tokyo 113-8657, Japan
[d] Department of Biophysics and Biochemistry, Graduate School of Science, The University of Tokyo, 7-3-1 Hongo, Bunkyo-ku, Tokyo 113-0033, Japan

ARTICLE INFO

Article history:
Received 3 September 2008
Available online 20 September 2008

Keywords:
Complex structure
Pleckstrin homology domain
Phosphatidylinositol
Membrane targeting
Dimerization

ABSTRACT

Bruton's tyrosine kinase (Btk) of the Tec family possesses a Pleckstrin homology (PH) domain, which is responsible for plasma membrane targeting. In this study, the crystal structure of the Btk PH domain in complex with dibutylyl-phosphatidylinositol-3,4,5-triphosphate was determined. The structure revealed that the Btk PH domain forms a homodimer and that each molecule binds phosphatidylinositol in the binding pocket. The side chain of Lys18 within a Btk-specific insertion in the β1–β2 loop is able to form a hydrogen bond with the diacylglycerol moiety of phosphatidylinositol. The other Btk-specific insertion in the β5–β6 loop constitutes the dimerization interface. Thus, the modes of phosphatidylinositol recognition and Btk PH domain dimerization are distinct from those of other PH domains.

Bruton's tyrosine kinase (Btk) gene mutations cause the immunodeficiency disease X-linked agammaglobulinemia in humans and X-linked immunodeficiency (Xid) in mice [1,2]. The disease is the result of a B-lymphocyte developmental defect, in which Btk-dependent signal transduction pathways are inactivated, and B cells remain at the pre-B cell stage. Btk belongs to the Tec family of non-receptor protein tyrosine kinases, whose members, Itk, Rlk, Tec, Btk, and Bmx, share a common domain construction [3]. In its N-terminal region, Btk possesses a Pleckstrin homology (PH) domain characteristically followed by the Tec homology (TH) domain. The TH domain contains a Zn^{2+} binding region, known as the Btk motif, and a proline-rich region. The C-terminal region contains a Src homology (SH) 2 domain, an SH3 domain, and a tyrosine kinase domain (Fig. 1A).

Lyn activates phosphatidylinositol 3-kinase following B cell receptor stimulation, and then phosphatidylinositol-3,4,5-triphosphate (PtdIns(3,4,5)P_3) is produced. Subsequently, Btk is recruited to the plasma membrane, where it interacts with PtdIns(3,4,5)P_3 [3]. The PH domain is responsible for binding with phosphoinositides and is important for the regulation of membrane recruitment [4,5]. The Btk PH domain recognizes PtdIns(3,4,5)P_3 more specifically than other phosphatidylinositols [6]. The crystal structures of the complexes between the PH domains and various ligands have revealed their specific binding in canonical [7–14] and non-canonical [15,16] manners. The crystal structure of the complex of the Btk PH domain with D-*myo*-inositol 1,3,4,5-tetrakisphosphate (Ins(1,3,4,5)P_4) revealed that the Btk PH domain recognizes Ins(1,3,4,5)P_4 in the canonical manner [7]. Most of such ligands are water soluble inositol phosphates, and discussions of phosphatidylinositol recognition have focused on the phosphate groups of the inositol ring. In addition, the affinity of the Btk PH domain for PtdIns(3,4,5)P_3 varies with different lipid lengths [6]. This implies that the Btk PH domain recognizes not only inositol phosphates but also the diacylglycerol moiety and/or the lipid. All of the crystal structures of the Btk PH domain have been determined as dimers, although it may be a monomer in solution [17]. Therefore, it is possible that the Btk PH domain dimerizes upon membrane binding and that its phosphatidylinositol recognition is important.

In the present study, we determined the crystal structure of a Btk fragment consisting of the PH domain and the Btk motif in complex

Abbreviations: SH, Src homology; PH, Pleckstrin homology; PtdIns(3,4,5)P_3, phosphatidylinositol-3,4,5-triphosphate; Ins(1,3,4,5)P_4, D-*myo*-inositol 1,3,4,5-tetrakisphosphate

* Corresponding author. Address: Systems and Structural Biology Center, Yokohama Institute, RIKEN, 1-7-22 Suehiro-cho, Tsurumi, Yokohama 230-0045, Japan. Fax: +81 45 503 9195.
E-mail address: yokoyama@biochem.s.u-tokyo.ac.jp (S. Yokoyama).
[1] Present address: Institute of Medical Chemistry, Hoshi University, 2-4-4-1 Ebara, Shinagawa, Tokyo 142-8501, Japan.

0006-291X/$ - see front matter © 2008 Elsevier Inc. All rights reserved.
doi:10.1016/j.bbrc.2008.09.055

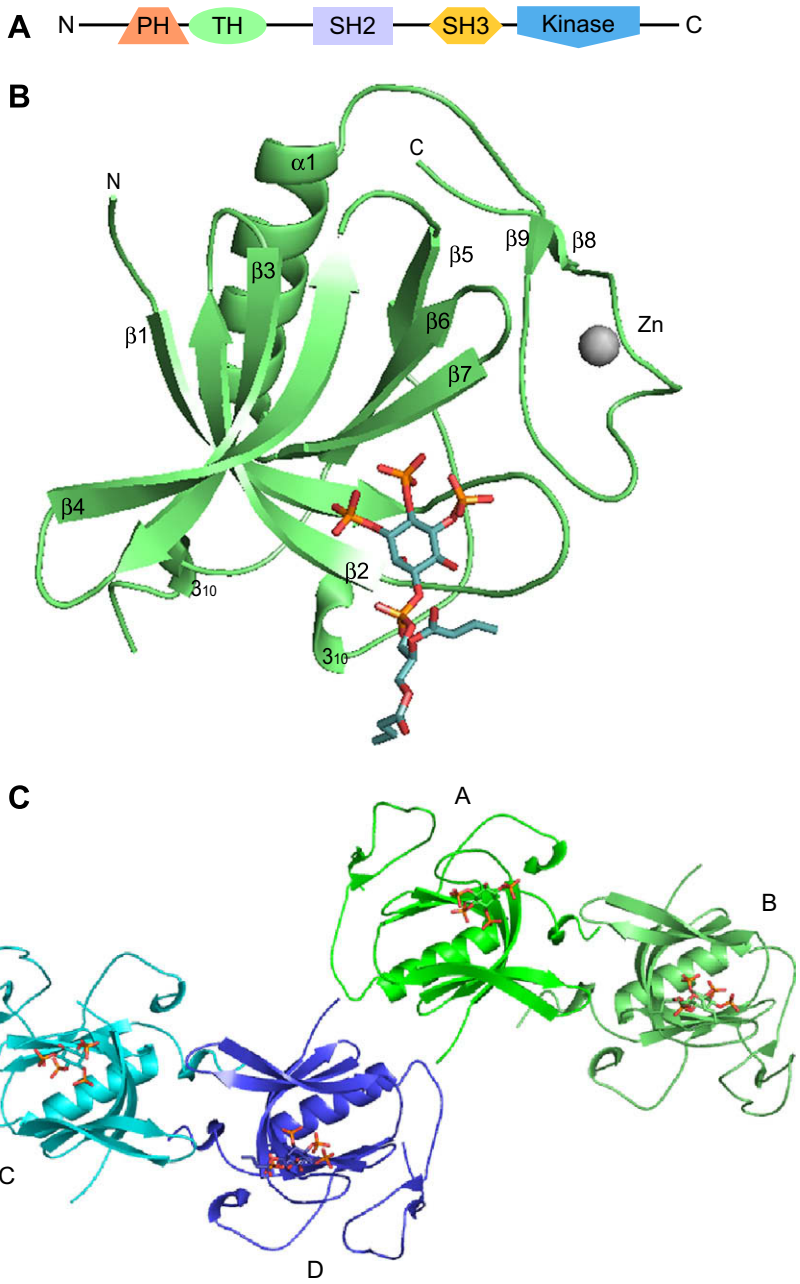

Fig. 1. (A) Schematic presentation of the domain architecture of Btk. (B) Ribbon representation of the crystal structure of the Btk PH domain (monomer structure, molecule B). The phosphatidylinositol molecule and the Zinc ion are drawn in a stick model and gray sphere, respectively. (C) Crystal structures of the Btk PH domains in the asymmetric unit.

with dibutylyl-phosphatidylinositol-3,4,5-triphosphate (C4PtdIns(3,4,5)P_3), to clarify the PtdIns(3,4,5)P_3 recognition and dimerization mechanisms. The electron density of C4PtdIns(3,4,5)P_3 was observed in the ligand binding sites of the two PH domain molecules, suggesting that the diacylglycerol moieties are involved in phosphatidylinositol recognition by the Btk PH domain dimer.

Materials and methods

Expression and purification. The Btk PH domain was expressed in *Spodoptera frugiperda* Sf9 insect cells using the baculovirus expression system. The cells were collected by centrifugation. After sonication, the insoluble components were removed by centrifugation (16,000*g*) for 60 min. The supernatant was loaded onto a HiTrap SP (GE Healthcare) column, equilibrated with 20 mM Tris–HCl buffer (pH 7.0) containing 100 mM NaCl and 1 mM DTT. The Btk PH domain was eluted by a linear gradient of 0–1 M NaCl. Btk PH domain-containing fractions were pooled and then loaded onto a Mono S (GE Healthcare) column, equilibrated with 20 mM Tris–HCl buffer (pH 7.0) containing 100 mM NaCl and 1 mM DTT, which was eluted by a linear gradient of 0–1 M NaCl. Fractions containing the protein were pooled and subjected to gel-filtration on a HiLoad Superdex75 (GE Healthcare) column equilibrated with 20 mM Tris–HCl buffer (pH 7.0), containing 100 mM NaCl and 1 mM DTT. Finally, the protein was concentrated to ~12.6 mg/ml with an Amicon ultra filter (Millipore).

Crystallization and data collection. The purified Btk PH domain and C4PtdIns(3,4,5)P_3 were co-crystallized by the hanging-drop vapor-diffusion method. The protein solution, at a final protein concentration of 6.3 mg/ml, was mixed with 0.5 mg/ml

C4PtdIns(3,4,5)P_3. The crystals were grown by equilibrating a mixture containing 1 μl of protein solution and 1 μl of reservoir solution (25% PEG 3350, 0.2 M lithium sulfate, 0.1 M MES buffer (pH6.5)). The plate-shaped crystals appeared within a few days, and grew to approximate dimensions of 0.1 × 0.1 × 0.05 mm. A data set collected on the beamline NW12 at the Photon Factory (Tsukuba, Japan) was processed and scaled with the HKL2000 suite [18]. Data collection statistics are presented in Table 1 (Supplementary material).

Structure determination and refinement. The crystal structure of the Btk PH domain in complex with C4PtdIns(3,4,5)P_3 was determined by Molecular Replacement (MR) with MOLREP, in the CCP4 program suite [19], using the structure of the unliganded form of the Btk PH domain (PDB ID:1BTK) as a search model.

The model was built manually into the electron density map, using O [20]. The structure was refined using the program CNS [21]. Since the loop regions (molecule A: 80–88, molecule B: 80–87, molecule C: 18–22 and 80–88, molecule D: 81–88) could not be identified in the electron density map due to disorder, these residues were not included in the subsequent refinement process. The final refinement statistics are shown in Table 1 (Supplementary material). The stereochemical quality of the final model was assessed using the program PROCHECK [22]. Figures were generated using the PyMOL program [23]. Atomic coordinates have been deposited in the Protein Data Bank, with the accession code 2Z0P.

Analytical ultracentrifugation. All analytical ultracentrifugation experiments were performed using a Beckman Optima XL-I analytical ultracentrifuge with an An-50 Ti rotor. The sample buffers were 20 mM Tris–HCl (pH 7.0), 100 mM NaCl and 5 mM β-mercaptoethanol (without C4PtdIns(3,4,5)P_3), and 10 mM Tris–HCl (pH 7.0), 50 mM NaCl, 2.5 mM β-mercaptoethanol and 0.46 mg/ml of C4PtdIns(3,4,5)P_3. All experiments were performed at 4 °C. Sedimentation equilibrium experiments were carried out with six-channel centerpieces, with loading concentrations of 0.94 mg/ml, 0.47 mg/ml and 0.24 mg/ml for both measurements. Data were obtained at 12,000, 14,000 and 16,000 rpm. A total equilibration time of 16 h was used for each speed, with scans taken at 12 and 14 h to ensure that equilibrium had been reached. The absorbance wavelength was 280 nm, and the optical baseline was determined by overspeeding at 40,000 rpm at the end of data collection. The equilibrium data were fitted using the manufacturer's software, XL-A/XL-I Data Analysis software version 6.03.

Results and discussion

Crystal structure

The crystal structure was determined as a complex with a water soluble analog, C4PtdIns(3,4,5)P_3. Overall, each monomer has an α-helix, α1, and nine β-strands, β1–β9 (Fig. 1B). The Btk PH domain adopts the common PH domain fold, with a seven-stranded antiparallel β-sheet, arranged into the β-sandwich, and the α1 helix. The following Btk motif is coordinated with a zinc ion, and is located in the vicinity of the β5–β7 strands. The crystal structure contains four molecules (molecules A–D) in the asymmetric unit (Fig. 1C). In a structural comparison among these molecules, the root mean square deviations (rmsd) revealed that each molecule is almost identical (rmsd = 0.257–0.477 Å). These four molecules contact each other by side-by-side interactions in the crystal packing. The phosphatidylinositol binding pockets are not involved in these side-by-side interactions. Molecules A and C expose the diacylglycerol moieties of C4PtdIns(3,4,5)P_3 to the solvent. In contrast, molecules B and D closely contact the symmetry-related neighbor molecules, and a broad electron density was observed for the diacylglycerol moieties of C4PtdIns(3,4,5)P_3. Thus, the diacylglycerol moieties in molecules B and D could be included in the structure refinement procedure (Fig. 2A).

The crystal structures of the Btk PH domains have been previously determined as the unliganded structure (PDB-ID:1BTK) [24] and the complex with Ins(1,3,4,5)P_4 (PDB-ID:1B55, 1BWN) [25]. The overall Btk PH domain fold in these previous structures is the same as ours in this report. The β5–β6 loop was partially disordered in our Btk PH domain structures and in the previous ones, except for one molecule in the unliganded Btk PH domain dimer structure.

Lipid binding

The three-dimensional structure of the complex between the Btk PH domain and C4PtdIns(3,4,5)P_3 revealed that the Btk PH domain binds the headgroup phosphoinositide in the canonical manner, in which the β1–β2 strands/loop and the β3–β4 strands play key roles in specific interactions [5]. The amino acid residues involved in these interactions are almost the same as those in the structure of the Btk PH domain in complex with Ins(1,3,4,5)P_4 [17]. As mentioned above, the aliphatic chains of C4PtdIns(3,4,5)P_3 were found for molecules B and D in the crystal structure, while the PtdIns(3,4,5)P_3 headgroups were observed for all four molecules. These headgroups of the C4PtdIns(3,4,5)P_3 molecules superimposed well, but the two observed diacylglycerol moieties adopted different conformations (Fig. 2B). Furthermore, the two aliphatic chains of each diacylglycerol moiety point in different directions. This indicates that the aliphatic chains of C4PtdIns(3,4,5)P_3 are too short to fix their orientations in the crystal structure. Since the actual long aliphatic chains *in vivo* (one is stearic acid and the other is arachidonic acid) are assembled in the same orientation to form a lipid bilayer, the carbonyl groups of the diacylglycerol moieties are likely to be facing the proteins, as in molecule B (Fig. 2C). Lys18 is close to the carbonyl group of the diacylglycerol moiety, although direct interactions were not found between them in the present structure. Assuming that the Lys18 side chain in molecule B adopts one of the possible rotamers ($\chi_1 = 62°$, $\chi_2 = 180°$, $\chi_3 = 180°$, $\chi_4 = 180°$) [25], the distance between the carbonyl oxygen of the diacylglycerol moiety and the ammonium group nitrogen of Lys18 would be less than 4.3 Å, which is short enough to form a hydrogen bond (Fig. 2C).

A structural comparison between the liganded and unliganded structures revealed the different conformations of the β1–β2 loop. In the unliganded structure (1BTK), the distance between the end of the β1–β2 loop (Cα carbon of Lys19) and the Btk motif (Cα carbon Gly150) is 4.6 Å, while that in the liganded structures (this work) is 12.7 Å. This conformational change, i.e. from "the open form" to "the closed form", is likely to take place naturally between the unliganded and liganded states. Consequently, the Btk PH domain can recognize not only the headgroup but also the diacylglycerol moieties of PtdIns(3,4,5)P_3 with conformational rearrangements. This mechanism may be supported by the observed specificity of the Btk PH domain for phosphoinositides: the affinity for C8PtdIns(3,4,5)P_3 is approximately 40 times higher than that for Ins(1,3,4,5)P_4 [6]. Furthermore, the Btk PH domain appears to have 5- to 6-fold higher affinity for C16PtdIns(3,4,5)P_3 than C8PtdIns(3,4,5)P_3 [6]. The longer aliphatic chain may stabilize a particular orientation of the diacylglycerol moiety in solution by micelle formation. The stabilized orientation of the diacylglycerol moiety may be favorable for its putative interaction with the Btk PH domain.

The β1–β2 loop contains three lysines (Lys17, 18, and 19). Although the side chain of Lys17 is located at a distance where it can interact with the PtdIns(3,4,5)P_3 headgroup, it forms an intramolecular salt bridge with Glu108. The K19E mutant is reportedly a loss-of-function mutant; however, it does not decrease the

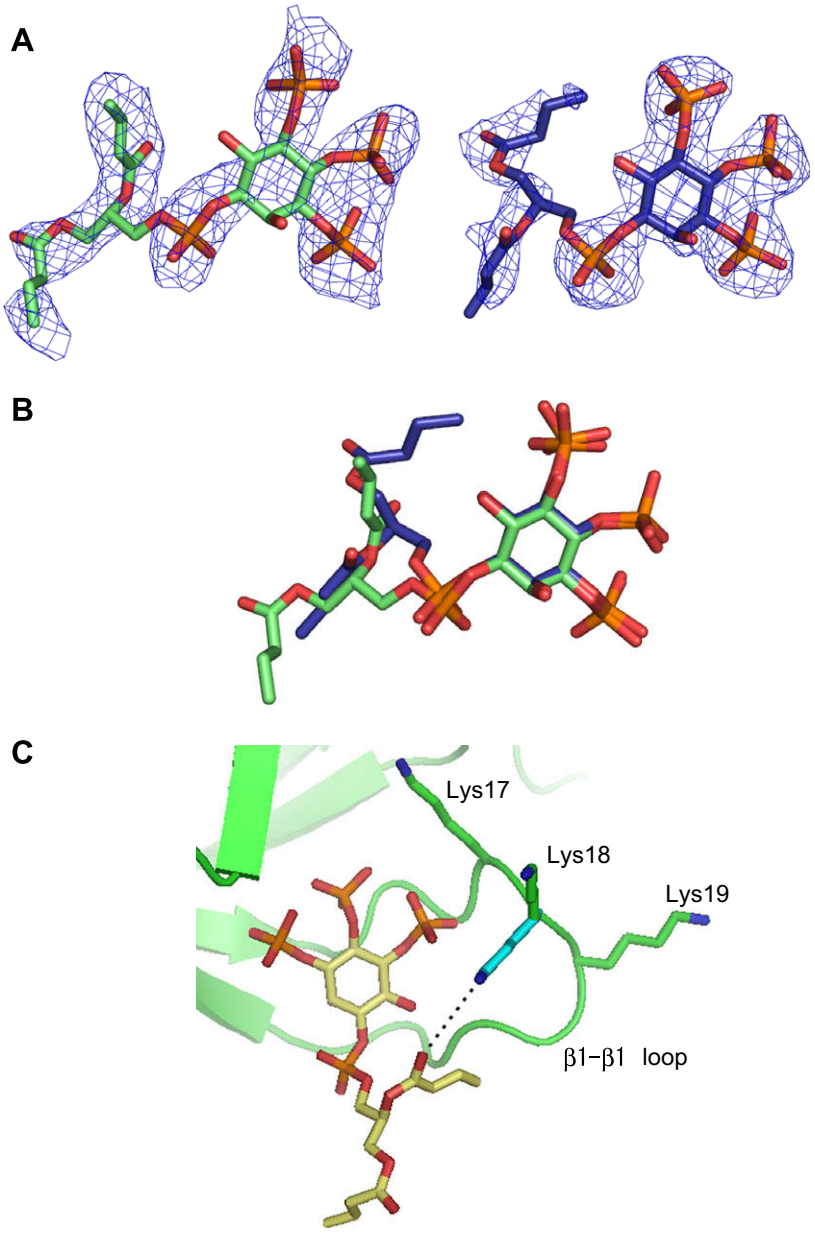

Fig. 2. (A) Fo-Fc omit maps and model fitting for phosphatidylinositol. The electron densities are contoured at 2.0σ. The carbon backbones are colored blue (molecule B) and green (molecule D), respectively. (B) Superposition of the phosphatidylinositol molecules. (C) Representation of the C4PtdIns(3,4,5)P_3 binding site. The three lysine residues (K17, 18 and 19) within the β1–β2 loop are depicted in stick models (green). The conformational change of Lys18 is drawn in cyan. The dotted line indicates a possible hydrogen bond.

binding affinity for either PtdIns(3,4,5)P_3 or Ins(1,3,4,5)P_4 [17]. This indicates that Lys19 does not bind to the same molecule of PtdIns(3,4,5)P_3 in the binding site, but to neighboring molecules of PtdIns(3,4,5)P_3 on the membrane surface. A comparison with other PH domains revealed that a short insertion exists in the β1–β2 loop of the Btk PH domain (Fig. 3). Lys17, 18 and 19 are included in this insertion. Therefore, a unique feature of the Btk PH domain is that the longer β1–β2 loop can simultaneously interact with multiple diacylglycerol groups of PtdIns(3,4,5)P_3.

Dimerization

An ultracentrifugation analysis revealed that the molecular masses of the Btk PH domain in solution are 23,012 Da with C4PtdIns(3,4,5)P_3 (20,821 Da; theoretical value as a monomer-C4PtdIns(3,4,5)P_3 complex) and 19,246 Da without C4PtdIns (3,4,5)P_3 (19,953 Da as a monomer). These values suggested that the Btk PH domain exists as a monomer in solution. This is consistent with the report that a dimer formation could not be detected in either the presence or absence of Ins(1,3,4,5)P_4 in solution [17]. In addition, a small angle X-ray scattering analysis showed that the full-length Btk is a monomer and assumes an elongated conformation in solution [26]. On the other hand, the crystal structure of the Btk PH–C4PtdIns(3,4,5)P_3 complex (this work) includes two dimers, with an assembled architecture almost identical to that of the Btk PH–Ins(1,3,4,5)P_4 complex structure. No significant structural differences were found between the liganded and unliganded structures, except for the conformation of the β1–β2 loop. The dimer interface involves the β3–β4 loop and a short helix between β5 and β6, in which Ile9, Tyr42, Phe44, Ile92, Ile94, and Ile95 form a hydrophobic core. A sequence alignment revealed that this region is not present in other PH do-

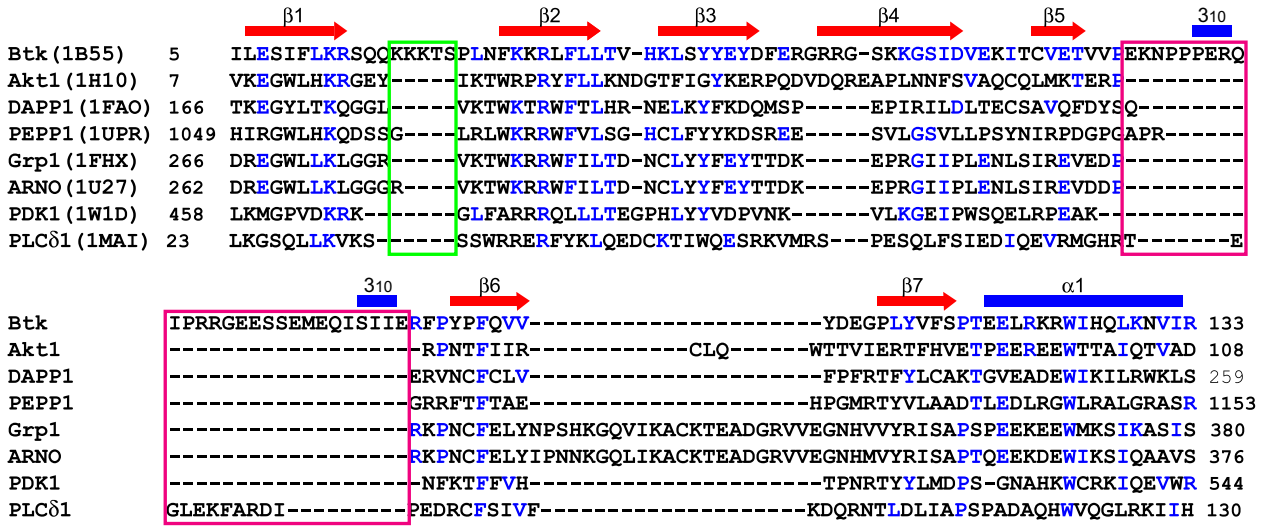

Fig. 3. Structure-based sequence alignment of the PH domains. The secondary structures of the Btk PH domain are displayed in blue bars (α-helices and 3_{10} helices) and red arrows (β-strands). Blue letters denote identically conserved amino acids with the Btk PH domain. The boxes indicate the insertion region in the β1–β2 loop (green) and the dimerization region (magenta) for the Btk PH domain.

mains (Fig. 3). This special insertion may have become adapted for Btk PH dimerization.

Although there have been no direct observations of dimerization, we propose that both the orientation and concentration are important for Btk PH domain dimerization on the membrane. The Btk molecules are recruited and concentrated on the membrane through interactions between the PH domain and PtdIns(3,4,5)P_3. These concentrated Btk molecules on the membrane are stably positioned by specific interactions, not only with the PtdIns(3,4,5)P_3 headgroup but also with the diacylglycerol moiety. These interactions consequently lead the contact surface on the PH domain to adopt the appropriate orientation and distance to form a dimer. Actually, the PtdIns(3,4,5)P_3 binding sites are arranged in the same orientation in the crystal structure. This dimerization process is distinctive for the Btk PH domain, due to (1) the unique insertion in the β1–β2 loop for interaction with PtdIns(3,4,5)P_3 and (2) the other insertion for the monomer-monomer interface.

Acknowledgments

This work was supported by Special Coordination Funds for Promoting Science and Technology, and the RIKEN Structure Genomics/Proteomics Initiative in the National Project on Protein Structural and Functional Analyses, Ministry of Education, Culture, Sports, Science and Technology. We thank Takako Fujimoto and Dr. Sumiko Gomi for their technical assistance in protein expressions.

Appendix A. Supplementary data

Supplementary data associated with this article can be found, in the online version, at doi:10.1016/j.bbrc.2008.09.055.

References

[1] J.M. Lindvall, K.E. Blomberg, J. Valiaho, L. Vargas, J.E. Heinonen, A. Berglof, A.J. Mohamed, B.F. Nore, M. Vihinen, C.I. Smith, Bruton's tyrosine kinase: cell biology, sequence conservation, mutation spectrum, siRNA modifications, and expression profiling, Immunol. Rev. 203 (2005) 200–215.
[2] J. Valiaho, C.I. Smith, M. Vihinen, BTKbase: the mutation database for X-linked agammaglobulinemia, Hum. Mutat. 27 (2006) 1209–1217.
[3] M. Felices, M. Falk, Y. Kosaka, L.J. Berg, Tec kinases in T cell and mast cell signaling, Adv. Immunol. 93 (2007) 145–184.
[4] M.A. Lemmon, Phosphoinositide recognition domains, Traffic 4 (2003) 201–213.
[5] J.P. DiNitto, D.G. Lambright, Membrane and juxtamembrane targeting by PH and PTB domains, Biochim. Biophys. Acta 1761 (2006) 850–867.
[6] L.E. Rameh, A. Arvidsson, K.L. Carraway 3rd, A.D. Couvillon, G. Rathbun, A. Crompton, B. VanRenterghem, M.P. Czech, K.S. Ravichandran, S.J. Burakoff, D.S. Wang, C.S. Chen, L.C. Cantley, A comparative analysis of the phosphoinositide binding specificity of pleckstrin homology domains, J. Biol. Chem. 272 (1997) 22059–22066.
[7] C.C. Milburn, M. Deak, S.M. Kelly, N.C. Price, D.R. Alessi, D.M. Van Aalten, Binding of phosphatidylinositol 3,4,5-trisphosphate to the pleckstrin homology domain of protein kinase B induces a conformational change, Biochem. J. 375 (2003) 531–538.
[8] S.J. Mills, D. Komander, M.N. Trusselle, S.T. Safrany, D.M. van Aalten, B.V. Potter, Novel inositol phospholipid headgroup surrogate crystallized in the pleckstrin homology domain of protein kinase Bα, ACS Chem. Biol. 2 (2007) 242–246.
[9] K.M. Ferguson, M.A. Lemmon, J. Schlessinger, P.B. Sigler, Structure of the high affinity complex of inositol trisphosphate with a phospholipase C pleckstrin homology domain, Cell 83 (1995) 1037–1046.
[10] K.M. Ferguson, J.M. Kavran, V.G. Sankaran, E. Fournier, S.J. Isakoff, E.Y. Skolnik, M.A. Lemmon, Structural basis for discrimination of 3-phosphoinositides by pleckstrin homology domains, Mol. Cell 6 (2000) 373–384.
[11] D. Komander, A. Fairservice, M. Deak, G.S. Kular, A.R. Prescott, C. Peter Downes, S.T. Safrany, D.R. Alessi, D.M. van Aalten, Structural insights into the regulation of PDK1 by phosphoinositides and inositol phosphates, EMBO J. 23 (2004) 3918–3928.
[12] C.C. Thomas, M. Deak, D.R. Alessi, D.M. van Aalten, High-resolution structure of the pleckstrin homology domain of protein kinase b/akt bound to phosphatidylinositol (3,4,5)-trisphosphate, Curr. Biol. 12 (2002) 1256–1262.
[13] S.E. Lietzke, S. Bose, T. Cronin, J. Klarlund, A. Chawla, M.P. Czech, D.G. Lambright, Structural basis of 3-phosphoinositide recognition by pleckstrin homology domains, Mol. Cell 6 (2000) 385–394.
[14] T.C. Cronin, J.P. DiNitto, M.P. Czech, D.G. Lambright, Structural determinants of phosphoinositide selectivity in splice variants of Grp1 family PH domains, EMBO J. 23 (2004) 3711–3720.
[15] D.F. Ceccarelli, I.M. Blasutig, M. Goudreault, Z. Li, J. Ruston, T. Pawson, F. Sicheri, Non-canonical interaction of phosphoinositides with pleckstrin homology domains of Tiam1 and ArhGAP9, J. Biol. Chem. 282 (2007) 13864–13874.
[16] M. Hyvonen, M.J. Macias, M. Nilges, H. Oschkinat, M. Saraste, M. Wilmanns, Structure of the binding site for inositol phosphates in a PH domain, EMBO J. 14 (1995) 4676–4685.
[17] E. Baraldi, K.D. Carugo, M. Hyvonen, P.L. Surdo, A.M. Riley, B.V. Potter, R. O'Brien, J.E. Ladbury, M. Saraste, Structure of the PH domain from Bruton's tyrosine kinase in complex with inositol 1,3,4,5-tetrakisphosphate, Structure 7 (1999) 449–460.
[18] Z. Otwinowski, W. Minor, Processing of X-ray diffraction data collected in oscillation mode, Methods Enzymol. 276 (1997) 307–326.
[19] N. Collaborative Computational Project, The CCP4 suite: programs for protein crystallography, Acta Crystallogr. D Biol. Crystallogr. 50 (1994) 760–763.
[20] T.A. Jones, J.Y. Zou, S.W. Cowan, M. Kjeldgaard, Improved methods for building protein models in electron density maps and the location of errors in these models, Acta Crystallogr. A 47 (1991) 110–119.

[21] A.T. Brunger, P.D. Adams, G.M. Clore, W.L. DeLano, P. Gros, R.W. Grosse-Kunstleve, J.S. Jiang, J. Kuszewski, M. Nilges, N.S. Pannu, R.J. Read, L.M. Rice, T. Simonson, G.L. Warren, Crystallography & NMR system: a new software suite for macromolecular structure determination, Acta Crystallogr. D Biol. Crystallogr. 54 (1998) 905–921.
[22] R.A. Laskowski, M.W. MacArthur, D.S. Moss, J.M. Thornton, PROCHECK: a program to check the stereochemical quality of protein structures, J. Appl. Crystallogr. 26 (1993) 283–291.
[23] W.L. DeLano, The PyMOL Molecular Graphics System, ed., (2002). Available from: <http://www.pymol.org>.
[24] M. Hyvonen, M. Saraste, Structure of the PH domain and Btk motif from Bruton's tyrosine kinase: molecular explanations for X-linked agammaglobulinaemia, EMBO J. 16 (1997) 3396–3404.
[25] S.C. Lovell, J.M. Word, J.S. Richardson, D.C. Richardson, The penultimate rotamer library, Proteins 40 (2000) 389–408.
[26] J.A. Marquez, C.I. Smith, M.V. Petoukhov, P. Lo Surdo, P.T. Mattsson, M. Knekt, A. Westlund, K. Scheffzek, M. Saraste, D.I. Svergun, Conformation of full-length Bruton tyrosine kinase (Btk) from synchrotron X-ray solution scattering, EMBO J. 22 (2003) 4616–4624.